Collecting back-reflected photons in photoacoustic microscopy

Hao F. Zhang[1,5], Jing Wang[1,3], Qing Wei[1], Tan Liu[1], Shuliang Jiao[2,4], and Carmen A. Puliafito[2]

[1]*Department of Electrical Engineering and Computer Science, University of Wisconsin-Milwaukee, Milwaukee WI 53201, USA*
[2]*Department of Ophthalmology, University of Southern California, Los Angeles, CA 90033, USA*
[3]*College of Electronic Science and Engineering, Jilin University, Changchun, 130012, China*
[4]*sjiao@usc.edu*
[5]*zhang25@uwm.edu*

Abstract: Since the photoacoustic effect relies only on the absorbed optical energy, the back-reflected photons from samples in optical-resolution photoacoustic microscopy are usually discarded. By employing a 2 × 2 single-mode fiber optical coupler in a laser-scanning optical-resolution photoacoustic microscope for delivering the illuminating laser light and collecting the back reflected photons, a fiber-optic confocal microscope is integrated with the photoacoustic microscope. Thus, simultaneous multimodal imaging can be achieved with a single light source and images from the two modalities are intrinsically registered. Such capabilities are demonstrated in imaging both phantoms and small animals *in vivo*.

OCIS codes: (110.5120) Photoacoustic imaging; (170.1790) Confocal microscopy; (110.0180) Microscopy.

References and Links

1. H. F. Zhang, K. Maslov, G. Stoica, and L. V. Wang, "Functional photoacoustic microscopy for high-resolution and noninvasive in vivo imaging," Nat. Biotechnol. **24**(7), 848–851 (2006).
2. A. De La Zerda, C. Zavaleta, S. Keren, S. Vaithilingam, S. Bodapati, Z. Liu, J. Levi, B. R. Smith, T. J. Ma, O. Oralkan, Z. Cheng, X. Y. Chen, H. J. Dai, B. T. Khuri-Yakub, and S. S. Gambhir, "Carbon nanotubes as photoacoustic molecular imaging agents in living mice," Nat. Nanotechnol. **3**(9), 557–562 (2008).
3. E. Z. Zhang, J. G. Laufer, R. B. Pedley, and P. C. Beard, "In vivo high-resolution 3D photoacoustic imaging of superficial vascular anatomy," Phys. Med. Biol. **54**(4), 1035–1046 (2009).
4. K. Maslov, H. F. Zhang, S. Hu, and L. V. Wang, "Optical-resolution photoacoustic microscopy for *in vivo* imaging of single capillaries," Opt. Lett. **33**(9), 929–931 (2008).
5. Z. X. Xie, S. L. Jiao, H. F. Zhang, and C. A. Puliafito, "Laser-scanning optical-resolution photoacoustic microscopy," Opt. Lett. **34**(12), 1771–1773 (2009).
6. L. V. Wang, "Multiscale photoacoustic microscopy and computed tomography," Nat. Photonics **3**(9), 503–509 (2009).
7. K. H. Song, C. H. Kim, C. M. Cobley, Y. N. Xia, and L. V. Wang, "Near-infrared gold nanocages as a new class of tracers for photoacoustic sentinel lymph node mapping on a rat model," Nano Lett. **9**(1), 183–188 (2009).
8. J. Laufer, E. Zhang, G. Raivich, and P. Beard, "Three-dimensional noninvasive imaging of the vasculature in the mouse brain using a high resolution photoacoustic scanner," Appl. Opt. **48**(10), D299–D306 (2009).
9. S. Jiao, R. Knighton, X. Huang, G. Gregori, and C. A. Puliafito, "Simultaneous acquisition of sectional and fundus ophthalmic images with spectral-domain optical coherence tomography," Opt. Express **13**(2), 444–452 (2005).
10. S. L. Jiao, Z. X. Xie, H. F. Zhang, and C. A. Puliafito, "Simultaneous multimodal imaging with integrated photoacoustic microscopy and optical coherence tomography," Opt. Lett. **34**(19), 2961–2963 (2009).
11. T. Dabbs, and M. Glass, "Fiber-optic confocal microscope: FOCON," Appl. Opt. **31**(16), 3030–3035 (1992).
12. M. Gu, *Principles of three-dimensional imaging in confocal microscopes* (Word Scientific, 1996).
13. E. Salomatina, B. Jiang, J. Novak, and A. N. Yaroslavsky, "Optical properties of normal and cancerous human skin in the visible and near-infrared spectral range," J. Biomed. Opt. **11**(6), 064026 (2006).
14. R. H. Webb, G. W. Hughes, and F. C. Delori, "Confocal scanning laser ophthalmoscope," Appl. Opt. **26**(8), 1492–1499 (1987).
15. D. A. Atchison, and G. Smith, *Optics of human eye* (Butterworth-Heinemann, 2000).

#120567 - $15.00 USD Received 30 Nov 2009; revised 31 Dec 2009; accepted 4 Jan 2010; published 11 Jan 2010

16. S. Schmitz-Valckenberg, M. Fleckenstein, A. P. Göbel, K. Sehmi, F. W. Fitzke, F. G. Holz, and A. Tufail, "Evaluation of autofluorescence imaging with the scanning laser ophthalmoscope and the fundus camera in age-related geographic atrophy," Am. J. Ophthalmol. **146**(2), 183–192 (2008).

1. Introduction

Photoacoustic microscopy (PAM) is one of the fastest-growing imaging technologies due to its unique capability to achieve high-spatial resolution imaging of optical absorption contrast in biological tissue. Two forms of PAM, ultrasonic-resolution PAM (UR-PAM) [1–3] and optical-resolution PAM (OR-PAM) [4,5], have been developed for different targeted applications.

UR-PAM depends on ultrasonic localization and usually has a spatial resolution from 15 μm to 100 μm, depending on the bandwidth and center frequency of the ultrasonic detector. Since ultrasonic scattering is two orders of magnitude weaker than optical scattering in biological tissue, UR-PAM exceeds the existing depth limit (~1 mm) of high-resolution optical imaging and can probe deep (up to 30 mm) into tissue [1,3]. Although the spatial resolution becomes worse, the depth-to-resolution ratio is usually kept around 100 [6]. Hence, UR-PAM aims at deep-tissue applications such as imaging of the sentinel lymph node for diagnosing breast cancer [7] and small animal brain imaging [8].

OR-PAM relies on optical focusing to provide lateral resolution (can be as high as a few micrometers) and the ultrasonic detection can be either strongly focused [4] or unfocused [5]. OR-PAM has the potential to be integrated with existing optical microscopic imaging modalities, such as optical coherence tomography (OCT) [9], confocal microscopy, and two-photon microcopy, to provide multimodal imaging with complementary contrasts.

The development of laser-scanning optical-resolution PAM (LSOR-PAM) [5] solved the incompatibility between OR-PAM and existing optical microscopy by eliminating the mechanical scanning of the optical and ultrasonic components. LSOR-PAM has been successfully fused with spectral-domain OCT [10] to achieve simultaneous imaging of the microvasculature and micro-anatomy in small animals *in vivo*, which laid the foundation for potential applications in ophthalmic imaging.

Here, we report on the integration of LSOR-PAM with a fiber-optic confocal microscope (FOCON) [11] to achieve multimodal imaging of both optical absorption and optical scattering contrasts. The axial resolution of the confocal microscopy was quantified both theoretically and experimentally. The complementary contrast was demonstrated in both phantoms and small animals *in vivo*.

2. Methods and materials

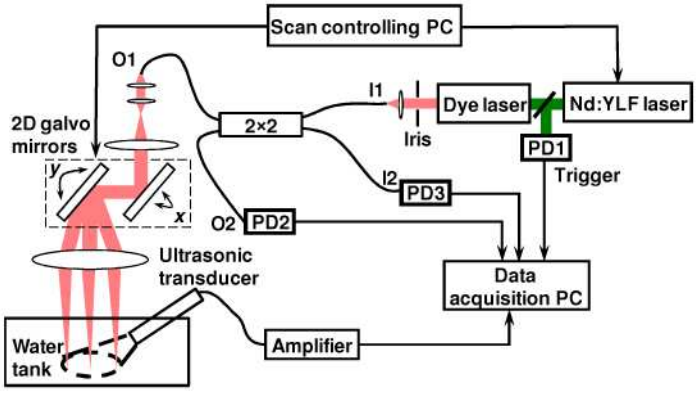

Fig. 1. Schematic of the fused laser-scanning confocal microscopy and photoacoustic microscopy. PD: photodiode; 2×2: fiber coupler.

#120567 - $15.00 USD Received 30 Nov 2009; revised 31 Dec 2009; accepted 4 Jan 2010; published 11 Jan 2010

Figure 1 shows a schematic of the experimental system. A tunable dye laser (Cobra, Sirah Laser and Plasmatchnik GmbH) pumped by a Nd:YLF laser system (IS8II-E, EdgeWave GmbH, pulse duration 6 ns, repetition rate: 1 kHz) was used as the irradiation source. The output wavelength was 578 nm. The laser light from the dye laser was spatially filtered by an iris and attenuated by a neutral density filter before coupled into a 2×2 single-mode optical fiber coupler (FC-632, Thorlabs). The output light from arm O1 was collimated and expanded to 10 mm in diameter and then scanned by a 2D galvanometer scanner (6230H, Cambridge Technology). An achromatic lens with a focal length of 40 mm (NT49-664, Edmund Optics) was used as the objective lens (please refer to Fig. 2(a) for more details). The output light from the second output arm O2 was detected by a photodiode (PD2, DET10A, Thorlabs) to record the energy of each laser pulse to compensate for the energy instability. The laser pulse energy out of the output arm O1 was 0.04 μJ.

The reflected light from the sample was detected by a 10-MHz Si photodiode (PD3, 2107-FC, New Focus) to form an FOCON image. A custom-built, high-frequency, unfocused ultrasonic transducer (center frequency: 40 MHz, active element size: 1 mm) detected the induced PA signals to form a PAM image. The data acquisition was triggered by laser pulses detected by PD1 (DET10A, Thorlabs) to avoid laser jittering.

This detection scheme permitted the natural integration of LSOR-PAM with FOCON, which allows simultaneous imaging the optical absorption and scattering contrasts without employing a second light source.

We applied the multimodal system to image the ears of a Swiss Webster mouse (body weight 20 g, Charles River Labs) *in vivo*. After the hairs on one of the ears were gently removed with commercial non-irritating hair removing lotion (Surgi Cream, Ardell), the animal was placed on a homemade animal holder for imaging. During experiments, a mixture of 1% isoflurane with medical grade oxygen was ventilated to the animal through a commercial non-rebreathing anesthesia system (M3000, LEI Medical) at a flow rate of 1 l/min to keep the animal motionless. All experimental animal procedures conformed to the laboratory animal protocol approved by the Animal Care and Use Committee of the University of Wisconsin–Milwaukee (UWM).

3. Results and discussions

3.1 Spatial resolution of LSOR-PAM

The lateral resolution of LSOR-PAM is determined by the size of the optical focus. As detailed in [5], the lateral resolution, which was 2.8 μm, approaches the diffraction limit of the objective lens at the illuminating wavelength (a detailed description of the numerical aperture is provided in the next section). The axial resolution is determined by the center frequency and bandwidth of the ultrasonic detector; this was quantified to be 23 μm using the "shift-and-sum" method as shown in [5].

3.2 Spatial resolution of FOCON

Figure 2(a) gives a detailed schematic of the optical illumination and detection in the FOCON. The optical fiber (SM600, Thorlabs) has a numerical aperture (NA) of 0.12 and a mode field diameter of 4.6 μm. The fiber collimator (PAF-X-7-A, Thorlabs) has a NA of 0.29 and an output beam waist diameter of 1.2 mm. The beam was further expanded to 10 mm in diameter before it was focused by the objective lens, which yields an objective NA of 0.125.

Because the optical fiber acts as the pinhole, the lateral resolution of FOCON improves from the lateral resolution of the LSOR-PAM and can be calculated as $k\lambda/NA$, where λ is the optical wavelength, NA is the numerical aperture of objective lens, k is a coefficient from 0.37 to 0.51 depending on the mode field radius of the optical fiber [11]. Taking $\lambda = 0.578$ μm, $NA = 0.125$, and the mode field radius of 2.3 μm, the lateral resolution of the confocal microscope is around 2 μm in air.

#120567 - $15.00 USD Received 30 Nov 2009; revised 31 Dec 2009; accepted 4 Jan 2010; published 11 Jan 2010

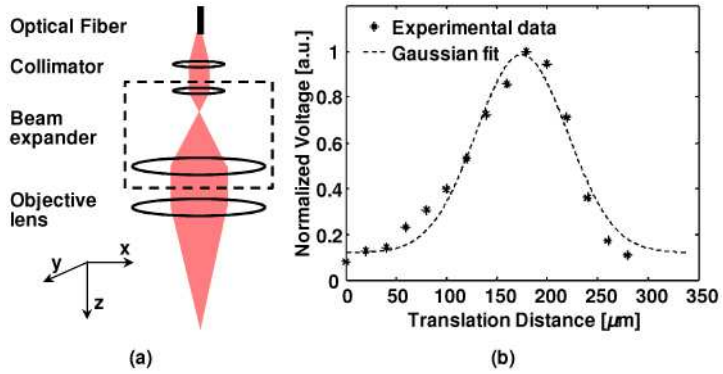

Fig. 2. Axial resolution of the confocal microscopy. (a) schematic of the optical illumination and detection for theoretical estimation; (b) experimental measurement of axial resolution.

The axial resolution of FOCON was first estimated theoretically. The axial resolution r can be expressed as $r = \lambda A/(\pi n NA_1^2)$ [12], where λ is the optical wavelength, n is the refractive index of the medium, NA_1 is the NA of the objective lens, A is the normalized fiber spot size and is expressed as $(2\pi r_0 NA_2)^2$, where r_0 is the mode field radius of the optical fiber and NA_2 is the minimum of the NA of the optical fibers and the collimating lens. Taking $\lambda = 0.578$ μm, $NA_1 = 0.125$, $r_0 = 2.3$ μm, and $NA_2 = 0.12$, we have $r = 106$ μm in air.

The axial resolution of FOCON in air was further quantified experimentally. A silver mirror was used as the sample and was translated along the z axis. A total distance of 300 μm was translated at a step size of 20 μm. The normalized reading from PD3 at each step is shown in Fig. 2(b). The experimental data were then fit by a Gaussian function $a\exp(-((x-b)/c)^2)+d$, where a, b, c, and d are unknown constants and d counts for the light reflection directly from the fiber tip of arm O1. The full-width-half-max (FWHM) value of the fitted Gaussian function gives the experimental measurement of axial resolution at 108 μm, which agrees with the theoretical estimation very well.

3.3 Phantom imaging

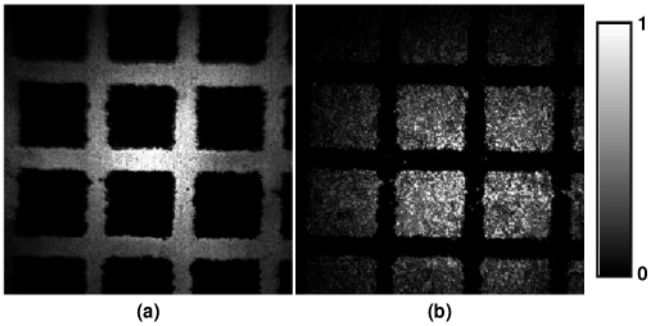

Fig. 3. Images of a printed mesh grid using the fused PAM and FOCON. (a) LSOR-PAM image; (b) FOCON image.

To demonstrate the complementary contrast of multimodal imaging, we imaged a printed mesh grid (grid size: 865 μm) as used in [1]. The grid has carbon lines on a printing transparency, where the dark lines have strong optical absorption. Figure 3 shows the imaging results. As can be observed, FOCON and PAM imaged opposite contrasts: the black printed lines induced strong PA signal [Fig. 3(a)] but very weak back-scattered photons for confocal microscopy [Fig. 3(b)] due to stronger optical absorption compared with the transparency. Since the LSOR-PAM and confocal microscopy share the same optical focus, the two images are intrinsically registered.

#120567 - $15.00 USD Received 30 Nov 2009; revised 31 Dec 2009; accepted 4 Jan 2010; published 11 Jan 2010

3.4 In vivo animal imaging

The *in vivo* images of a mouse ear are shown in Fig. 4. Because the source of optical absorption is mainly hemoglobin and the Swiss Webster mouse has low skin melanin concentration, LSOR-PAM revealed the anatomy of microvessels [Fig. 4(a)] well. Sebaceous glands are embedded in the dermis and have higher optical absorption compared with the dermis; hence, they create shadows in the LSOR-PAM image, as highlighted by arrows.

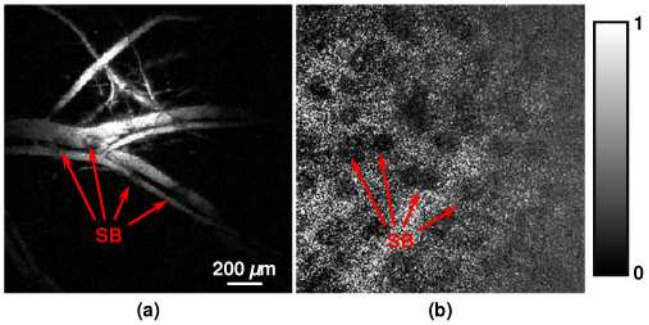

Fig. 4. *In vivo* multimodal imaging of a mouse ear. (a) LSOR-PAM image showing microvasculature; (b) FOCON image showing skin structure. SB: sebaceous gland.

Completely different anatomical features are observed in the FOCON image [Fig. 4(b)]. The detected photons are primarily reflected from epidermis and dermis. Since the sebaceous gland is more optically absorptive compared with the dermal tissue, fewer photons were back-reflected and the glands appeared to be dark regions in the image, which agrees with other reported results [13]. As highlighted in Fig. 4, the spatial locations of the glands correspond well in the two images. The contrast-to-noise ratios of the LSOR-PAM and FOCON images are 36 dB and 12 dB, respectively, which clearly demonstrates the advantage of LSOR-PAM when optical absorption contrast dominates. We noticed that blood vessels do not manifest themselves as dark regions in the FOCON image. It is, presumably, because that LSOR-PAM relies on only single-trip photon propagation while FOCON requires round-trip photons propagation and thus has less sensitivity in order to image blood vessels without contrast agents at a low NA.

4. Conclusion

The novelty of this work comes from the integration, for the first time, of confocal microscopy with photoacoustic microscopy based on shared optical delivery, optical scanning, and light source for multimodal imaging. The significance of this work is that it exhibits the feasibility of integrating LSOR-PAM with the well-established confocal scanning laser ophthalmoscope (cSLO) [14] for potential multimodal ophthalmic imaging based on a single light source. The 0.125 NA of the objective lens used in this study was specifically chosen to be close to the optical parameters of human eyes [15]. Although not demonstrated experimentally, this system is readily expandable to conduct confocal fluorescence microscopy [16] by adding appropriate band-pass filters and a high-sensitivity optical detector (such as a photon multiplication tube), yet still sharing the same light source with LSOR-PAM.

Acknowledgments

This work is supported in part by the UWM start-up fund, the UWM Research Growth Initiative grant, the Shaw Scientist Award, and the Juvenile Diabetes Research Foundation Innovative Grant 5-2009-498 to H. F. Zhang. Support is also provided in part by the National Institutes of Health grant 7R21EB008800-02 to S. Jiao. Both H. F. Zhang and S. Jiao are corresponding authors to this paper.

#120567 - $15.00 USD Received 30 Nov 2009; revised 31 Dec 2009; accepted 4 Jan 2010; published 11 Jan 2010